diagnostics

MDPI

Review

Musculoskeletal Manifestations of Sickle Cell Disease: What the Radiologist Should Know

Amin Aboultaif [1], Ahmed Alsooreti [2], Ahmad Alnaggar [2,3], Khalid Khan [2] and Rola Husain [4,*]

[1] Royal College of Surgeons of Ireland, Medical University of Bahrain-RCSI—MUB, Busaiteen 228, Bahrain
[2] Salmaniya Medical Complex, Governmental Hospitals, Manama, Bahrain; ahmed.alsoorti@gmail.com (A.A.)
[3] Zagazig University Hospital, Zagazig 44519, Egypt
[4] Dubai Hospital, Dubai Health, Mohammed Bin Rashid University of Medicine and Health Sciences, Dubai P.O. Box 505055, United Arab Emirates
* Correspondence: rola.mahmood@gmail.com

Abstract

Objective: To review the musculoskeletal manifestations of sickle cell disease (SCD), using Bahraini patients as an example, and raise awareness among radiologists and non-radiologist physicians of these imaging findings to facilitate early recognition and improve patient outcomes through timely medical or surgical management. **Materials and Methods:** This review analyzes findings from previous studies on musculoskeletal manifestations of SCD using various imaging modalities, including plain radiography, CT, MRI, and ultrasound. Specific attention was given to marrow changes, avascular necrosis, septic arthritis, osteomyelitis, and other complications. These findings were subsequently identified in Bahraini patients by searching the radiology information system (RIS) at the main public hospital in Bahrain, and representative images were selected for presentation in this review. **Results:** Musculoskeletal abnormalities in SCD arise from marrow hyperplasia, red marrow reconversion, and extramedullary hematopoiesis. Vaso-occlusive crises can lead to bone infarctions, osteomyelitis, and septic arthritis, which present unique diagnostic challenges. Pediatric patients often develop sickle cell dactylitis, while spontaneous hematomas are less common but have significant complications. **Conclusion:** Early recognition of SCD-related musculoskeletal manifestations is crucial for accurate diagnosis and effective management. Radiologists in high-prevalence regions must familiarize themselves with these findings to contribute to comprehensive, multidisciplinary treatment strategies that optimize patient outcomes.

Keywords: musculoskeletal manifestations; radiograph; ultrasound; computed tomography; MRI; osteonecrosis; osteomyelitis

Academic Editor: Mara Carsote

Received: 8 September 2026
Revised: 20 October 2026
Accepted: 21 October 2026
Published: 27 November 2026

Copyright: © 2026 by the authors. Licensee MDPI, Basel, Switzerland. This article is an open access article distributed under the terms and conditions of the Creative Commons Attribution (CC BY) license.

1. Introduction

Sickle cell disease (SCD) is an inherited blood disorder characterized by the production of red blood cells, which become sickle-shaped or crescent-shaped [1–3]. This disease affects millions of people globally, with a significant prevalence among individuals of African, Mediterranean, Middle Eastern, and South Asian ancestry. Historically, the sickle cell trait first emerged in West and Central Africa centuries ago and later spread to regions including the Mediterranean, the Persian Gulf, parts of India, and eventually across the

Atlantic [4]. SCD is particularly common in Middle Eastern Arab countries, with an estimated 5000 new cases reported in 2005 [2]. In Bahrain, figures from 2002 have shown a birth prevalence of 0.9% for SCD and 16.3% for sickle cell trait [2]. Genetic variants of SCD are described in the literature depending on the geographic/ethnic origin of the genetic mutation. Possible haplotypes include the Central African Republic (CAR), Senegal (SEN), Cameroon (CAM), and the Arab-Indian haplotype (ARAB), which is the most prevalent haplotype seen in Bahrain [1].

The primary cause of SCD is a mutation in the β-chain of hemoglobin, leading to the production of hemoglobin S (Hb S) [1–3]. This mutation involves the substitution of glutamic acid with valine in the β-globin gene located on chromosome 11 [3–5]. As a result, abnormal sickle-shaped red blood cells are formed, which have an irregular shape and a higher breakdown rate, leading to vaso-occlusive attacks and anemia [3]. These musculoskeletal manifestations can result in further complications such as dactylitis, osteonecrosis, osteomyelitis, growth retardation, and ultimately skeletal deformities [3,4,6–8]. This paper discusses the musculoskeletal manifestations of SCD, particularly with a focus on the genetic Arab-Indian haplotype.

Images for this review article were acquired by searching the radiology information system (RIS) at the Salmaniya Medical Complex, the main public hospital in Bahrain, for the period from 2020–2026, using the search terms: sickle cell disease, sickle, and SCD. Representative images were subsequently obtained from the hospital's Picture Archiving and Communication System (PACS) after acquiring the approval of the research committee at the hospital.

1.1. Effects of Intramedullary Marrow Hyperplasia

SCD produces various musculoskeletal abnormalities as a result of chronic anemia. These include marrow hyperplasia and bone marrow reconversion, and occasionally, extramedullary hematopoiesis [5,8,9]. These alterations can be observed through imaging studies; for example, on radiographs, constant red blood cell production can result in osteopenia along with coarsening of the normal trabecular pattern seen in both the long and flat bones (Figure 1). On MRI, the normal fatty marrow, which elicits high signal intensity on both T1-WI and T2-WI, is replaced by red marrow, which returns intermediate signal intensity on T1-WI that remains higher than or equal to the skeletal muscles, sparing the epiphysis [10,11] (Figure 2). These changes could be focal in some instances and could be misdiagnosed as a sinister lesion, and thus necessitate further imaging with further special sequences such as in-phase (IP)/out-of-phase (OOP) sequences, where it should show reduction of signal intensity reflecting fatty content and confirming its benign nature [10].

The replacement of the red marrow could result in pathological fractures, as it weakens the bone, mainly due to the widening of the medullary spaces and thinning of the cortical bone due to the constant red blood cell production [5,9,12]. If the spine is involved, thinning of the cortex and softening of the bone create smooth anomalous biconcave vertebral bodies that characteristically give off the "fish-mouth" appearance on radiographs. Severe cases can result in vertebral collapse with kyphosis [9,12] (Figure 3). This progressive spinal deformity, seen in conditions with prolonged marrow expansion, affects structural support and increases the risk of vertebral fractures [9,12]. Bone marrow expansion in the skull manifests as the widening of the diploic space and the thinning of the inner and outer tables. If osteoporosis in the skull occurs, a granular appearance may be seen on radiographic images, along with a vertical projection of "hair-on-end" stripes seen in the outer aspect of the vault [9,12].

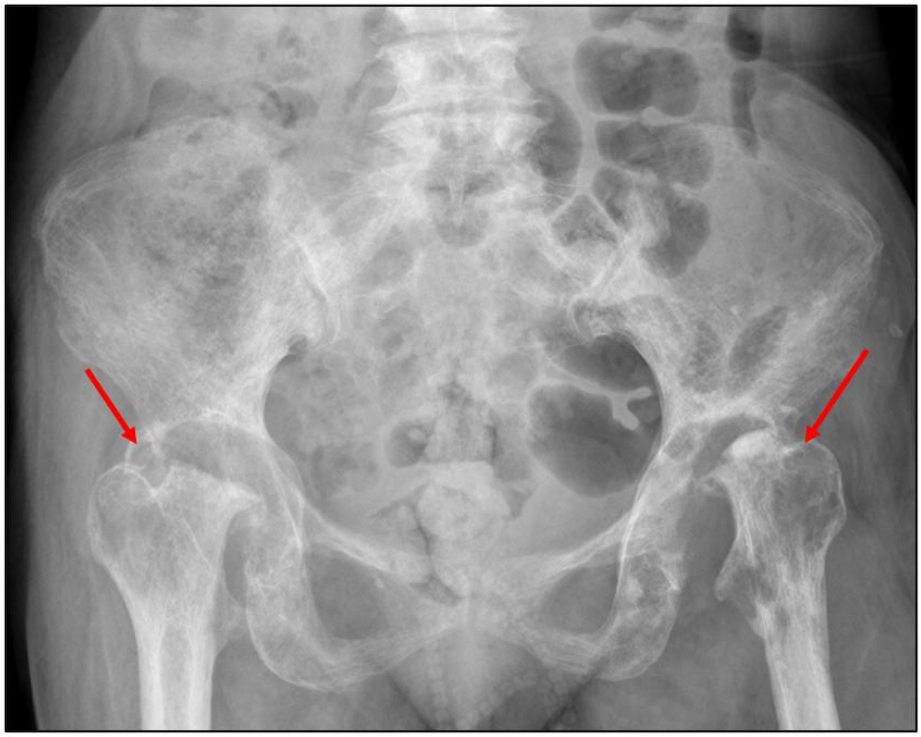


Figure 1. A known case of sickle cell disease with the radiograph revealing diffuse increased bony sclerosis and trabeculation reflecting sickle cell changes. Also note the destructive changes involving both hip joints (arrows), in keeping with septic arthritis.



Figure 2. MR images of a known case of sickle cell disease with right shoulder pain show: (**A**) Coronal T1-WI and (**B**) Coronal T2-weighted short inversion time inversion recovery (STIR) MR images show diffuse bone marrow reconversion (evidenced by heterogeneous STIR signal intensity with intermediate T1W signal intensity, relatively sparing the epiphysis: asterisks) and heterogeneous serpentine low T1WI and STIR signal intensity of the right humeral head surrounded by edema, in keeping with right humeral head avascular necrosis (arrows).

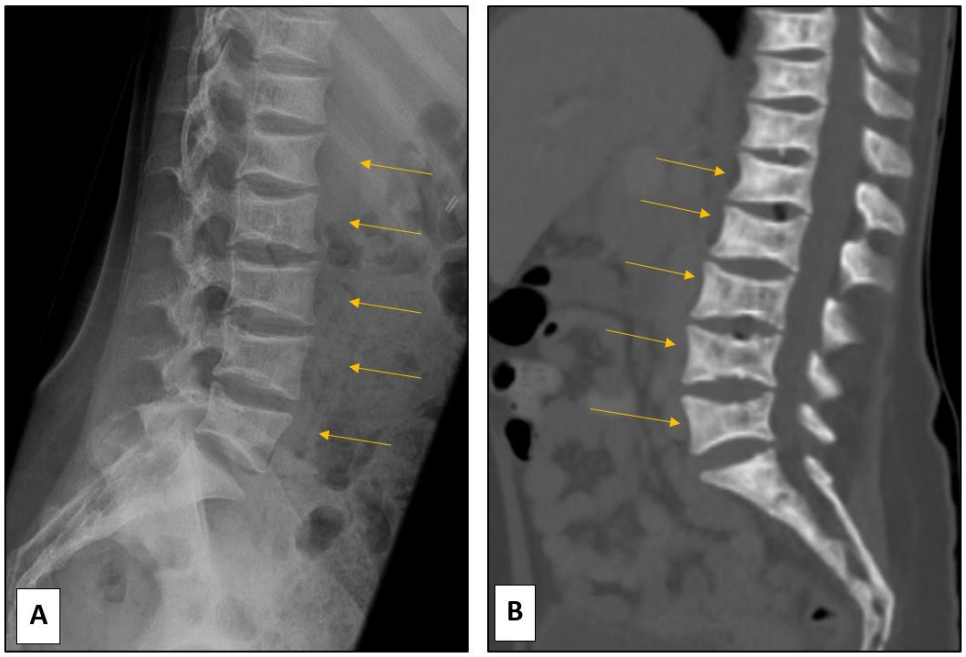


Figure 3. Lateral plain radiograph of lumbar spine (**A**) shows generalized osteopenia and multilevel central endplate depression (arrows). CT reformatted sagittal view for the same patient (**B**) exhibits generalized bony sclerosis and redemonstrates the multilevel central endplate depression giving the H-shaped appearance (arrows).

1.2. Extramedullary Hematopoiesis

Extramedullary hematopoiesis reflects a process in which blood cells are produced outside the bone marrow. It can present as soft tissue masses due to increased red blood cell (RBC) production in different body sites [13]. Extramedullary hematopoiesis, evident on computed tomography (CT) and magnetic resonance imaging (MRI), is frequently identified within the paraspinal intrathoracic regions, occasionally mimicking masses that require careful differentiation from malignancies; therefore, clinical history and laboratory correlation are crucial in order to make this distinction [14].

1.3. Osteonecrosis

Bone infarctions are serious and common complications in SCD. Children with SCD frequently exhibit sickle cell dactylitis (hand-foot syndrome), which manifests as soft tissue swelling around the digits and is a hallmark finding in younger patients [8]. This condition is often accompanied by spontaneous soft tissue hematomas, which can be challenging to distinguish from infections on ultrasound and MRI [8]. In long bones, bone infarctions and bone marrow edema typically appear on MRI as patchy, hyperintense regions on T2-WI or STIR (short tau inversion recovery) sequences, particularly during vaso-occlusive crises [15]. Avascular necrosis is osteonecrosis that affects the epiphysis. The most often affected areas are the femoral (Figures 4–7) and humeral heads (Figure 2) [11,16,17]. Eventually, reactive sclerosis and new bone formation develop in the infarcted regions of the medullary bone as well. Intramedullary sclerosis is characterized by metaphyseal or diaphyseal osteonecrosis [11,16,17] (Figure 8). Avascular necrosis in SCD can manifest diffusely, and lesions on MRI typically appear more prominent than those in other conditions [11,16,17].

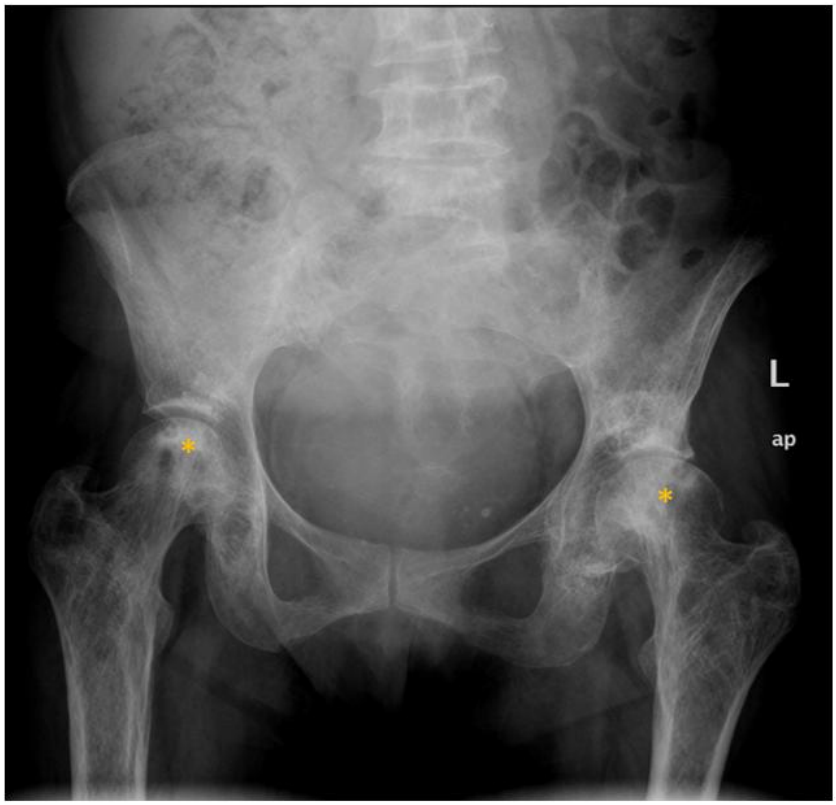


Figure 4. A case of SCD with thickened and coarse trabecula with features of bilateral femoral head osteonecrosis (asterisks).

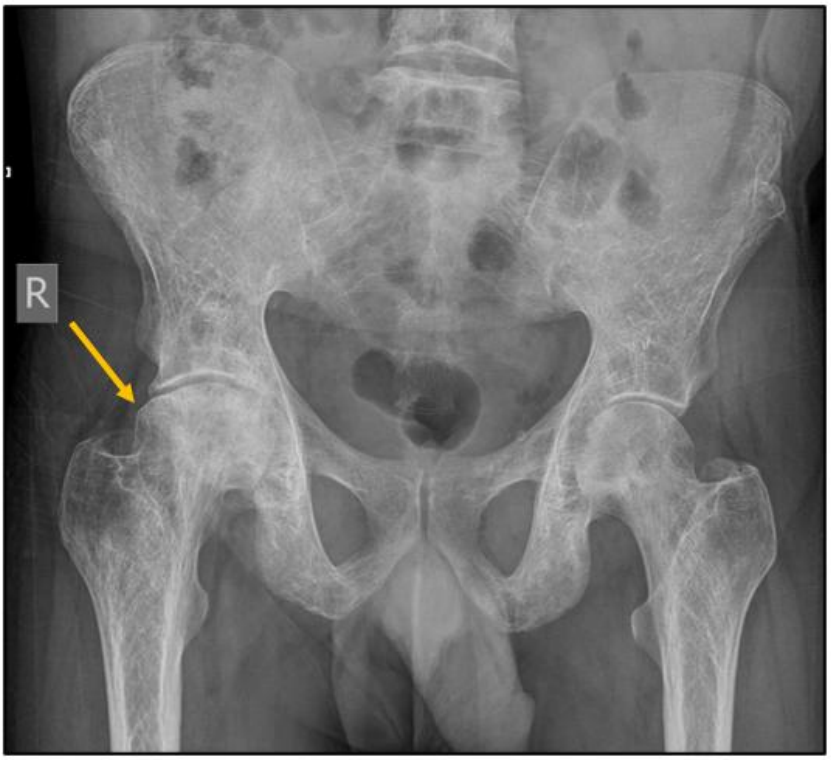


Figure 5. Frontal plain radiograph of the pelvis shows thickened trabecular pattern and coxa magna deformity of the right femoral head with deformity and flattening of the femoral head, in keeping with chronic right femoral head avascular necrosis (arrow).

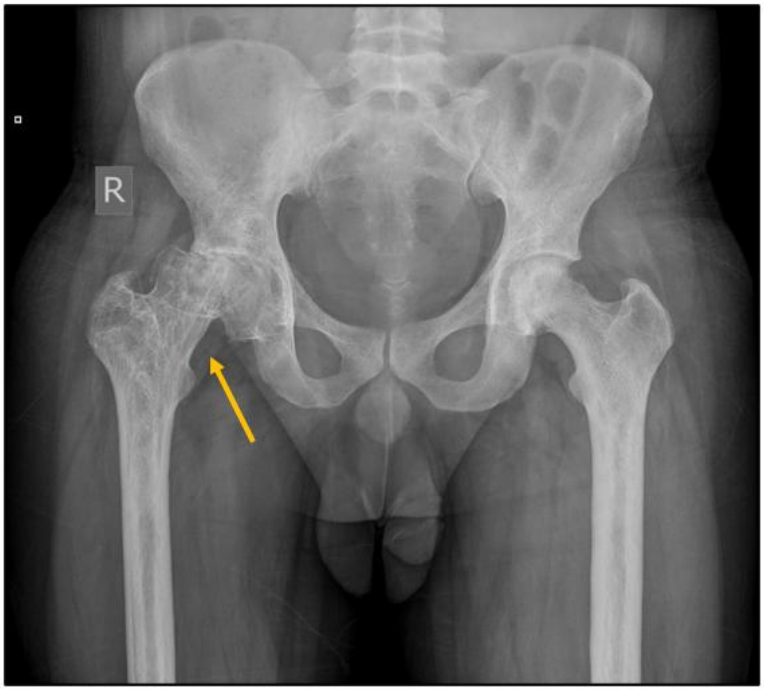


Figure 6. A case of hip pain in SCD, with the right hip showing evidence of advanced osteonecrosis with degenerative changes and subluxation of the hip joint (arrow).

Children with hyperplastic marrow have been shown to have stunted growth, with early epiphyseal closure, and asymmetrical and defective long bone formation [11,16,17]. The ischemia of the central vertebral growth plate can impact vertebral growth, causing the squared-off depression of the vertebral endplates to produce H-shaped vertebrae and, occasionally, the production of "tower" vertebrae as the height of the vertebrae increases without a corresponding increase in girth [11,16,17]. Adult patients more commonly show signs of advanced complications, such as avascular necrosis (AVN), particularly of the femoral and humeral heads, which appear as irregular joint surfaces and subchondral sclerosis on MRI [18] (Figures 4–7).

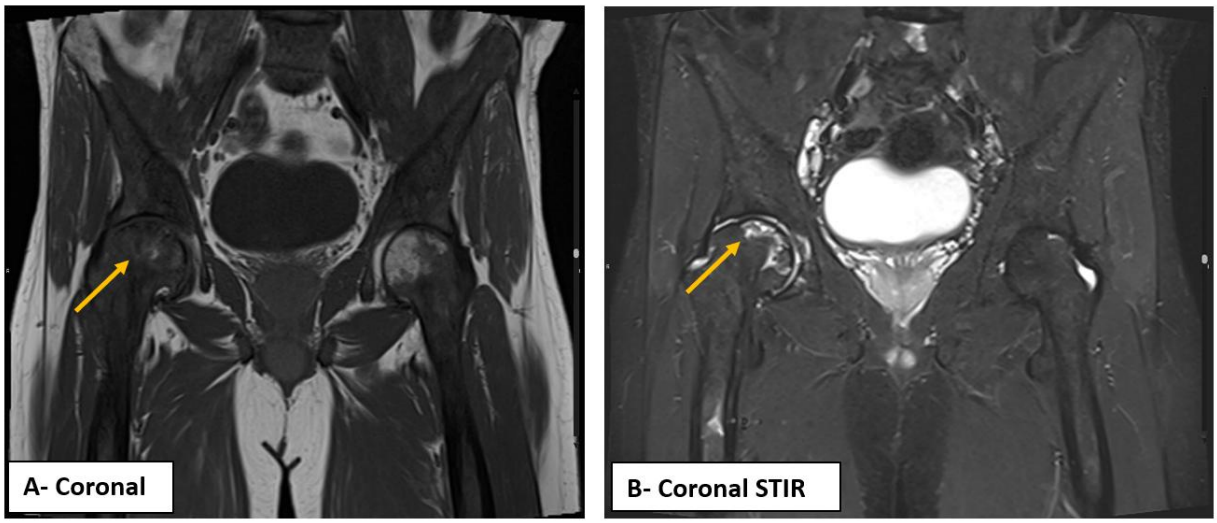


Figure 7. MRI of the same patient: (**A**) Coronal T1-WI and (**B**) Coronal T2-weighted short inversion time inversion recovery (STIR) MR images show diffuse bone marrow reconversion (evidenced by heterogeneous STIR signal intensity with intermediate T1W signal intensity, sparing the epiphysis)

and heterogeneous high STIR signal intensity of the right femoral head and articular surface flattening, confirming right femoral head avascular necrosis (arrows).



Figure 8. Multifocal serpentine heterogeneous signal intensity on coronal T1WI (**A**) and sagittal T1 post-contrast (**B**), compatible with bony infarctions.

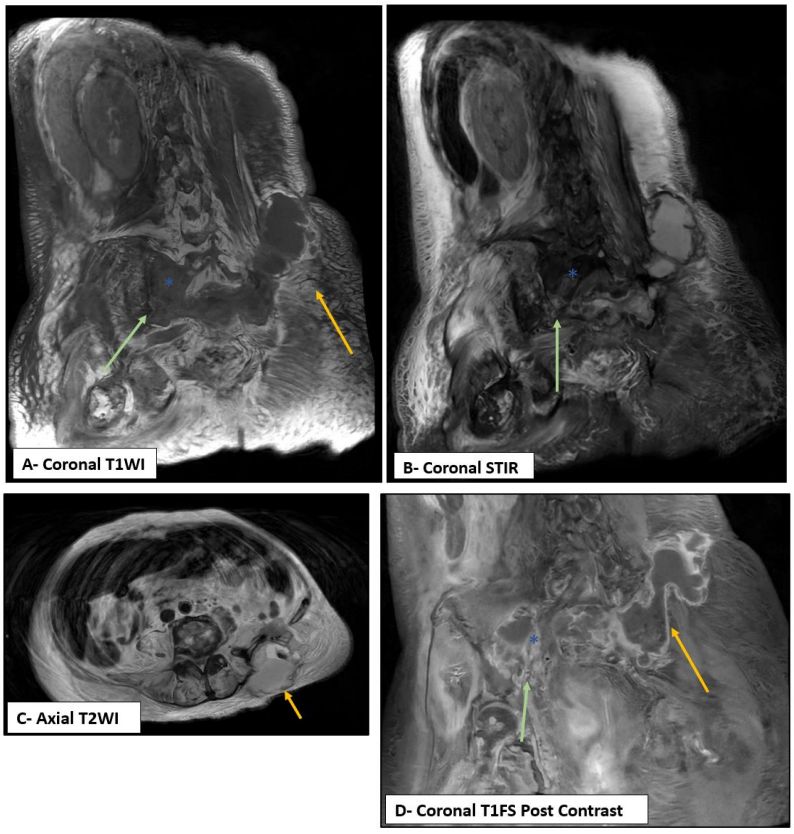
1.4. Osteomyelitis

Researchers identified several factors that make sickle cell disease patients more susceptible to musculoskeletal infections, including hyposplenism, reduced complement activity, and infarcted or necrotic bone [19]. Osteomyelitis is common in the pediatric population, and hence, early diagnosis and treatment can prevent complications such as bone destruction and deformity [20]. The diaphyses of small tubular bones in the hands and feet are usually affected in infants and young children, usually between 6 months and 2 years, due to the presence and persistence of red marrow [19]. They may result in sickle cell dactylitis or "hand-foot" syndrome.

Other documented complications of sickle cell disease include septic arthritis (Figures 9 and 10), often caused by *Salmonella* or *Staphylococcus* infections, which are visually distinguishable by their intense signal changes and joint effusions on MRI [8,11,16,17]. These infections necessitate swift intervention to prevent joint destruction, as seen in cases of osteomyelitis affecting long bones [21]. Pathological fractures are also common, especially in weight-bearing bones, where MRI and CT scans reveal cortical thinning and deformities secondary to repeated infarction and bone weakening [22]. Studies also highlight the correlation between specific genetic haplotypes, like the Arab-Indian haplotype, and distinct radiological manifestations, suggesting that genetic variation in SCD patients may influence the extent and type of skeletal abnormalities observed [6]. A vaso-occlusive crisis can cause ischemia, infarction, and severe pain, often affecting long bones, muscles, and digits. While infarctions are sometimes diagnosed incidentally on radiographs, infections may complicate diagnosis due to pre-existing changes [20]. These infections may spread directly via leg ulcers or through skin commensals (e.g., *Staphylococcus aureus* in the Middle East and Africa, and gram-negative bacilli such as *Salmonella* in America [23]), or hematogenously in the case of enteric bacteria, as sickling within the mesenteric vessels

can result in gastrointestinal infarction, which in turn can lead to osteomyelitis or septic arthritis [9,19,20,23,24]. The reduced blood supply in infarcted parts of the medullary bone might lead to a locally compromised immune response, and these areas can serve as an ideal environment for the growth of bacteria [11,16,17]. Additionally, phagocytosis, asplenia, and decreased complement activity may be another source of bone and joint infections in these patients, as they weaken the immune system [11,16,17]. Radiographic abnormalities are frequently non-specific and lag behind the osseous changes despite plain films frequently being the first line of imaging for osteomyelitis [11,16,17]. Given that osseous radiographic changes might not show up for the first 7–14 days, including but not limited to periostitis and regional osteopenia, especially in the pediatric population, other diagnostic tools might be more useful at this stage, including ultrasound, which may be able to delineate subperiosteal soft tissue thickening and, in later stages, subperiosteal collection, soft tissue abscess, identify joint effusion, and further aid in the process of image-guided aspiration and drainage [11,16,17,25]. The first radiographic changes may include blurring of fat planes and cortical bone, followed by cortical destruction, along with periosteal reaction (generally showing an aggressive appearance, such as hair-on-end or Codman triangle), endosteal scalloping, osteopenia, and loss of trabecular bony architecture [24,26–29] (Figure 11).

Overall, equivocal radiographic results usually mandate further investigation with cross-sectional imaging, as poor sensitivity for early identification and poor specificity of findings are frequently found in the presence of underlying chronic alterations such as osteonecrosis and arthritis [24,26–29]. CT plays a pivotal role in diagnosing cases of chronic osteomyelitis by identifying the bony changes manifested by the formation of sequestrum and involucrum, with sensitivity and specificity of 67% and 50%, respectively. These values increased with the addition of intravenous contrast to further delineate soft tissue abscesses [24,26–29] (Figure 12).



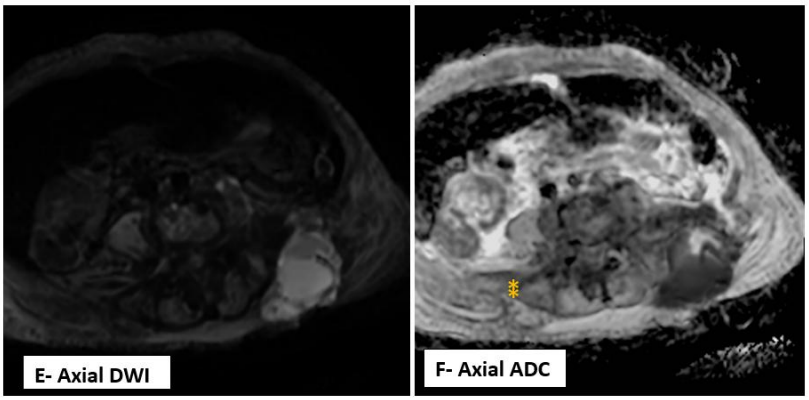


Figure 9. MRI showing bilateral sacroiliac joint septic arthritis (green arrows: evidenced by joint effusion and subchondral edema with enhancement on post-contrast images) and sacral osteomyelitis (blue asterisks: evidenced by low T1WI, with edema and enhancement on post-contrast images) with multifocal enhancing collections/abscess formations (yellow arrows: evidenced by fluid collections with enhancement and diffusion restriction (yellow asterisks)) with *Salmonella* found in multiple peripheral blood samples.

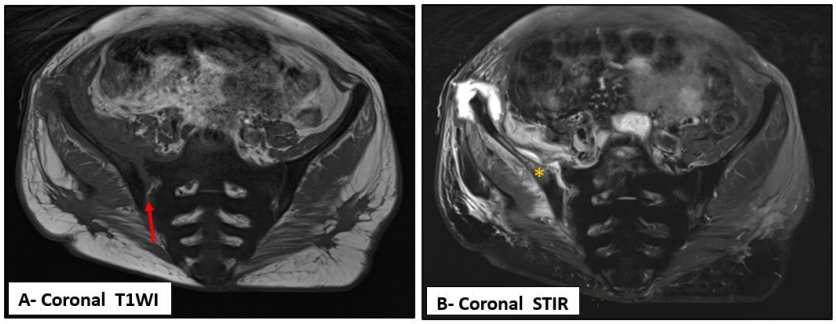


Figure 10. A known case of sickle cell disease with pain, with MRI revealing right-sided iliac osteomyelitis and sacroiliac joint septic arthritis in the form of unilateral widening and irregularity (arrow) of the right sacroiliac joint, with the joint fluid decompressing anteriorly deep to the iliacus muscle, forming a large localized collection, associated with edema, erosion, and destruction of the right iliac bone, deep to the collection, in keeping with osteomyelitis (asterisk). Note the dark signal of the bone marrow, due to the development of hemosiderosis, as a result and complication of recurrent blood transfusions.



Figure 11. Frontal plain radiograph of the left leg shows sickle cell skeletal changes with tunnel-shaped soft tissue lucency and haziness, along with periosteal reaction of the subjacent medial aspect of the proximal third of tibial diaphysis.

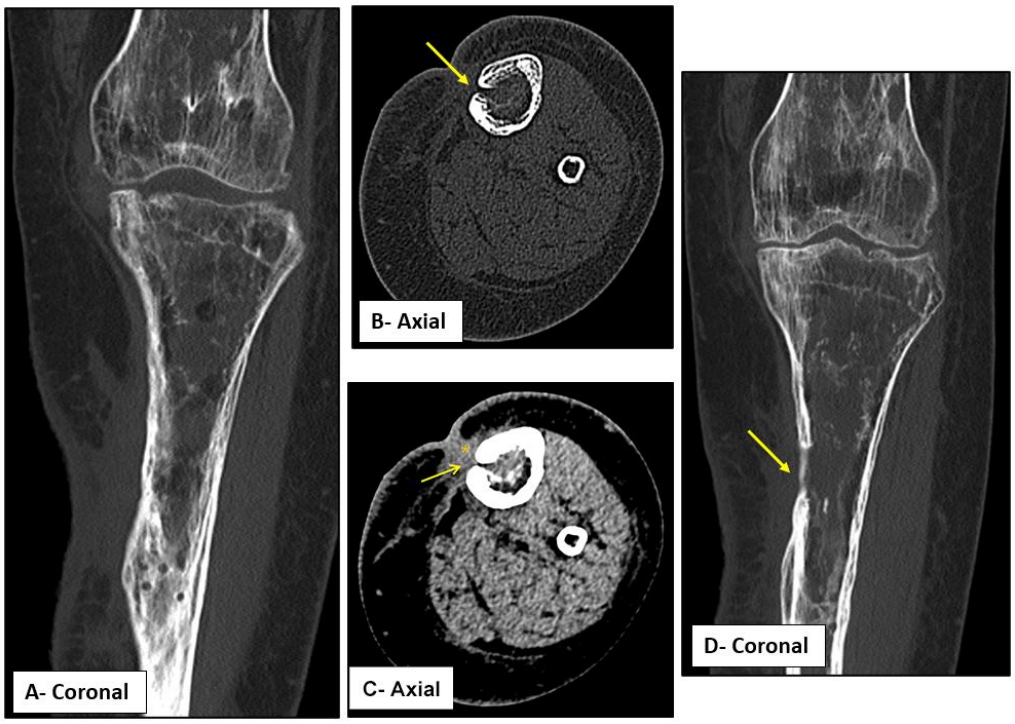


Figure 12. CT scan of the leg showing features of chronic osteomyelitis, characterized by inhomogeneous osteosclerosis of the tibia with a cortical defect (yellow arrows: cloaca), and a soft tissue sinus tract connecting it to the overlying skin (asterisk).

On MRI, osteomyelitis is characterized by regions of increased signal intensity within the bone marrow on T2-WI and STIR sequences, typically exhibiting ill-defined margins [24,26–29]. Using gadolinium-enhanced T1-WI with fat suppression yields the highest sensitivity and specificity, revealing abnormal enhancement patterns and potential periosteal or soft tissue involvement [30] (Figure 13). Additional MR sequences, such as diffusion-weighted images (DWI/ADC), by delineating areas of diffusion restriction, can further help make the distinction between infected and non-infected tissue in the correct clinical context [31] (Figure 9). Nonetheless, marrow infarction can present similarly on MRI, sharing overlapping characteristics such as elevated signal intensity on T2-WI and localized post-contrast enhancement, complicating the diagnostic process [24,26–29]. Scintigraphy utilizing isotopes such as indium-111, technetium-99m, and gallium-67 may be useful in certain clinical scenarios [32]. Additionally, clinical correlation manifested in raised inflammatory markers (ESR: erythrocyte sedimentation rate, CRP: C-reactive protein, WBC (white blood cell)/neutrophil count), along with cultures obtained from biopsy specimens may further aid in distinguishing between infection and infarction [24,26–29]. Table 1 compares the differentiating characteristics between osteonecrosis and osteomyelitis across the different imaging modalities [26–31].

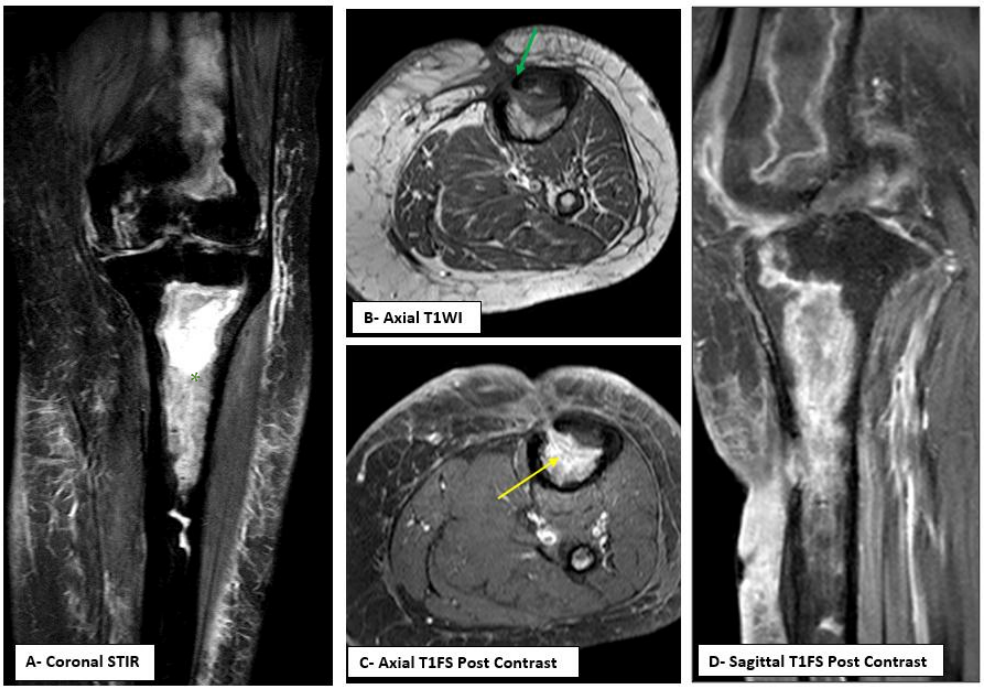


Figure 13. MRI of the same patient, showing: (**A**) Coronal STIR and (**B**) axial T1-WI show diffuse bone marrow reconversion with medullary infarction (asterisk), soft tissue swelling and marrow edema with an anterior cortical and subcutaneous defect (cloaca) (green arrow), (**C**) Axial T1-WI post-contrast image shows enhancing bone marrow (yellow arrow) and subcutaneous tissue consistent with acute on top of osteomyelitis and overlying soft tissue inflammation (**C**,**D**).

Table 1. Comparing the differentiating characteristics between osteonecrosis and osteomyelitis across the different imaging modalities.

Imaging Modality	Osteonecrosis	Osteomyelitis
Radiography	Variable appearance: • Normal • Ill-defined radiolucency • Mixed lucency and sclerosis	Changes might not show up for the first 7–14 days: • Periostitis • Regional osteopenia • Blurring of fat planes and cortical bone • Cortical destruction • Aggressive periosteal reaction • Endosteal scalloping and loss of trabecular bony architecture
Ultrasound	No defining features	• Subperiosteal soft tissue thickening • Subperiosteal collection (later stage) • Soft tissue abscess • Joint effusion if infection involves the joint
CT	Similar to radiography	• Important for diagnosing chronic osteomyelitis • Formation of sequestrum, involucrum • Soft tissue abscesses
MRI	• T1-WI: high signal centrally following fat signal • T2-WI: Geographic low signal rim, high signal inner rim (double line sign), Central fat signal	• T1-WI: Low signal • T2-WI, STIR: High signal intensity with ill-defined margins

	• Gadolinium-enhanced T1-WI with fat suppression: No abnormal marrow enhancement • DWI/ADC: No diffusion restriction	• Gadolinium-enhanced T1-WI with fat suppression: Abnormal enhancement ± periosteal or soft tissue (highest sensitivity and specificity for diagnosis) • DWI/ADC: May demonstrate diffusion restriction
Nuclear Medicine	No activity	• Can show increased activity with isotopes such as indium-111, technetium-99m, and gallium-67

1.5. Spontaneous Hematoma

Spontaneous hematomas are a rarely encountered manifestation of SCD in the pediatric population, and if they occur, they usually involve the facial bones and cranium and are associated with epidural bleeding. These could be treated conservatively, or depending on the severity, may mandate surgical intervention [24,26–29,33]. Many theories behind the pathophysiology of this condition are found in the literature, rooting back to the aforementioned bony changes seen in sickle cell patients, including bony infarction and chronic medullary hematopoiesis with the expansion of red bone marrow, all of which affect the periosteum and the overlying vessels, resulting in blood extravasation. Sickling of the RBC may also result in impaired venous flow, which may consequently result in hemorrhage [33–36].

The appearance on imaging varies depending on the age of hematoma: an acute hematoma is hyperdense on CT, iso- to hypointense on T1-WI, and hypointense on T2-WI on MRI, due to intracellular deoxyhemoglobin, and as it matures, it becomes isodense on CT in the subacute phase, while on MRI it shows slightly increased T1 and reduced T2 signal intensity in the early subacute phase (3–7 days), reflecting intracellular methemoglobin, and within the late subacute stage (1 week to 2–3 weeks), it exhibits high T1 and T2 signal, attributed to extracellular methemoglobin, along with diffusion restriction on DWI [33–36]. Lastly, in the chronic stage, the hematoma becomes isodense on CT scan, resembling CSF attenuation, while it may show peripheral low signal intensity on both T1 and T2-WI due to the accumulation of hemosiderin, with signal normalization on DWI [33–36] (Figure 14).

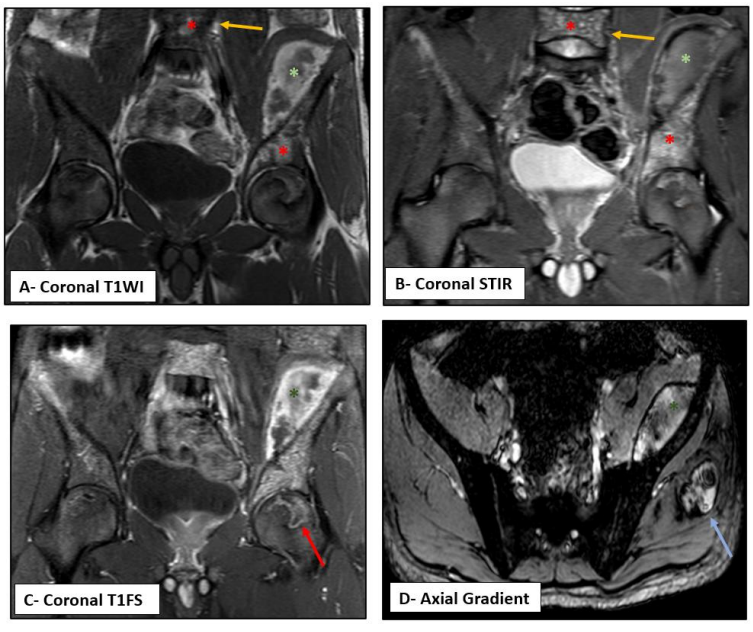


Figure 14. A case of vaso-occlusive attack with stigmata of sickle cell disease in the form of extensive marrow reconversion, H-shaped vertebrae (yellow arrow), medullary infarcts (red asterisks) involving the imaged pelvic and femoral bones, and bilateral avascular necrosis of the femoral heads (red

arrow), with no evidence of subchondral collapse. A localized fluid collection (green asterisks) deep to the left iliacus muscle is seen, exhibiting heterogeneous signal intensity on the visualized sequences, showing high signal intensity on T1 and T2 weighted images with heterogeneous enhancement on the postcontrast images, while blooming on the gradient weighted images. The signal characteristics reflect blood and blood products of different ages, in keeping with subiliacus hematoma. Note the left intramuscular gluteal hematoma (blue arrow).

As diagnosis becomes challenging in cases of sickle cell disease, where pathology overlaps with pre-existing infarction and red bone marrow changes as well as infection, susceptibility-weighted images such as T2*/SWI may be of great help by denoting the blooming artifacts, compatible with hemosiderin products, allowing for the differentiation between hematomas and pre-existing marrow changes [37,38].

2. Conclusions

Sickle cell disease is a genetic disorder with a relatively higher incidence and prevalence in Bahrain in particular and in the Middle East and Africa in general. The disease affects the skeletal system in variable ways, resulting in marrow changes, osteomyelitis, osteonecrosis, and spontaneous subperiosteal hematomas, among other complications. Recognizing acute events such as osteomyelitis amid the pre-existing background bone marrow and cortical changes remains a daily challenge to radiologists practicing in high-prevalence regions. Being able to recognize these features and their extent can aid in forming treatment plans and avoiding unnecessary imaging follow-up and interventions.

Author Contributions: Conceptualization, R.H. and A.A. (Ahmad Alnaggar); methodology, R.H.; validation, R.H. and A.A. (Ahmed Alsooreti); formal analysis, R.H.; investigation and curation, A.A. (Amin Aboultaif), A.A. (Ahmed Alsooreti), A.A. (Ahmad Alnaggar), K.K. and R.H.; writing—original draft preparation, R.H. and A.A. (Amin Aboultaif); writing—review and editing, R.H. and A.A. (Ahmed Alsooreti); supervision, R.H.; project administration, R.H. and A.A. (Ahmad Alnaggar). All authors have read and agreed to the published version of the manuscript.

Funding: This research received no external funding.

Institutional Review Board Statement: The study was conducted in accordance with the Declaration of Helsinki and approved by the Institutional Review Board of the Salmaniya Medical Complex–Bahrain (Research approval serial is IRB 114281123 and date of approval is 28 November 2023).

Informed Consent Statement: Patient consent was waived by the Institutional Review Board due to it is a pictorial review.

Data Availability Statement: The original contributions presented in this study are included in the article. Further inquiries can be directed to the corresponding author. No data from the included patients have been published previously in any journal nor is it currently under consideration for publication elsewhere. However, the data have been presented as a poster at the society of skeletal radiology meeting 2024.

Acknowledgments: The authors would like to thank Dubai Health for the financial support towards the article processing fee.

Conflicts of Interest: The authors declare no conflicts of interest.

Abbreviations

The following abbreviations are used in this manuscript:

SCD	Sickle cell disease
MRI	Magnetic resonance imaging

CT	Computed tomography
RBC	Red blood cells

References

1. El-Hazmi, M.A.; Al-Hazmi, A.M.; Warsy, A.S. Sickle cell disease in Middle East Arab countries. *Indian J. Med. Res.* **2011**, *134*, 597–610.
2. Al Arrayed, S. Campaign to control genetic blood diseases in Bahrain. *Public Health Genom.* **2005**, *8*, 52–55.
3. Loggetto, S.R. Sickle cell anemia: Clinical diversity and beta S-globin haplotypes. *Rev. Bras. DE Hematol. E Hemoter.* **2013**, *35*, 155–157.
4. Vaishya, R.; Agarwal, A.K.; Edomwonyi, E.O.; Vijay, V. Musculoskeletal manifestations of sickle cell disease: A review. *Cureus* **2015**, *7*, e358.
5. Al Hajeri, A.; Ali, M.; Saleh, L.; Alkowari, S.; Al Saad, A. Evaluation of Satisfaction Level of Sickle Cell Disease Patients Regarding the Healthcare Services in Bahrain: A Cross-sectional Study. *J. Bahrain Med. Soc.* **2019**, *31*, 10–16.
6. Ware, H.E.; Brooks, A.P.; Toye, R.; Berney, S.I. Sickle cell disease and silent avascular necrosis of the hip. *J. Bone Jt. Surg. Br. Vol.* **1991**, *73*, 947–949.
7. Elendu, C.; Amaechi, D.C.; Alakwe-Ojimba, C.E.; Elendu, T.C.; Elendu, R.C.; Ayabazu, C.P.; Aina, T.O.M.; Aborisade, O.M.; Adenikinju, J.S. Understanding sickle cell disease: Causes, symptoms, and treatment options. *Medicine* **2023**, *102*, e35237.
8. Ejindu, V.C.; Hine, A.L.; Mashayekhi, M.; Shorvon, P.J.; Misra, R.R. Musculoskeletal manifestations of sickle cell disease. *Radiographics* **2007**, *27*, 1005–1021.
9. Mourshed, F.; Tuckson, C.R. A study of the radiographic features of the jaws in sickle-cell anemia. *Oral Surg. Oral Med. Oral Pathol.* **1974**, *37*, 812–819.
10. Rajakulasingam, R.; Saifuddin, A. Focal nodular marrow hyperplasia: Imaging features of 53 cases. *Br. J. Radiol.* **2020**, *93*, 20200206.
11. Mallon, D.; Doig, D.; Dixon, L.; Gontsarova, A.; Jan, W.; Tona, F. Neuroimaging in sickle cell disease: A review. *J. Neuroimaging* **2020**, *30*, 725–735.
12. Sebes, J.I.; Diggs, L.W. Radiographic changes of the skull in sickle cell anemia. *Am. J. Roentgenol.* **1979**, *132*, 373–377.
13. Kosaraju, V.; Harwani, A.; Partovi, S.; Bhojwani, N.; Garg, V.; Ayyappan, S.; Kosmas, C.; Robbin, M. Imaging of musculoskeletal manifestations in sickle cell disease patients. *Br. J. Radiol.* **2017**, *90*, 20160130.
14. Chan, B.Y.; Gill, K.G.; Rebsamen, S.L.; Nguyen, J.C. MR imaging of pediatric bone marrow. *Radiographics* **2016**, *36*, 1911–1930.
15. Jain, R.; Sawhney, S.; Rizvi, S.G. Acute bone crises in sickle cell disease: The T1 fat-saturated sequence in differentiation of acute bone infarcts from acute osteomyelitis. *Clin. Radiol.* **2008**, *63*, 59–70.
16. Horvai, A.E.; Link, T.M. *Bone and Soft Tissue Pathology*; Elsevier Health Sciences: Amsterdam, The Netherlands, 2012.
17. Chang, A.K.; Ginter Summarell, C.C.; Birdie, P.T.; Sheehan, V.A. Genetic modifiers of severity in sickle cell disease. *Clin. Hemorheol. Microcirc.* **2018**, *68*, 147–164.
18. Khedr, S.A.; Hassaan, M.A.; Shabana, A.A.; Gaballah, A.H.; Mokhtar, D.A. Musculoskeletal manifestations of sickle cell disease, diagnosis with whole body MRI. *Egypt. J. Radiol. Nucl. Med.* **2012**, *43*, 77–84.
19. Musowoya, R.M.; Kaonga, P.; Bwanga, A.; Chunda-Lyoka, C.; Lavy, C.; Munthali, J. Predictors of musculoskeletal manifestations in paediatric patients presenting with sickle cell disease at a tertiary teaching hospital in Lusaka, Zambia. *Bone Jt. Open* **2020**, *1*, 175–181.
20. Urish, K.L.; Cassat, J.E. Staphylococcus aureus osteomyelitis: Bone, bugs, and surgery. *Infect. Immun.* **2020**, *88*, 10.1128.
21. Ganguly, A.; Boswell, W.; Aniq, H. Musculoskeletal manifestations of sickle cell anaemia: A pictorial review. *Anemia* **2011**, *2011*, 794283.
22. Bedair, E.M.A.; Almaslamani, N.J.; Yassin, M. Radiological manifestation of avascular necrosis (AVN) in sickle cell disease (SCD): A review of diagnostic imaging. *Acta Bio Medica Atenei Parm.* **2023**, *94*, e2023177.
23. Al Farii, H.; Zhou, S.; Albers, A. Management of osteomyelitis in sickle cell disease. *JAAOS Glob. Res. Rev.* **2020**, *4*, e20.
24. Pineda, C.; Espinosa, R.; Pena, A. Radiographic imaging in osteomyelitis: The role of plain radiography, computed tomography, ultrasonography, magnetic resonance imaging, and scintigraphy. In *Seminars in Plastic Surgery*; © Thieme Medical Publishers: New York, NY, USA, 2009; Volume 23, pp. 080–089.
25. Adam, M.; Musa, M.J.; Al-Qahtani, S.M.; Alelyani, M.; Musa, A.; Elzaki, M.; Alzain, A.F.; Ali, S.; Medani, A.; Mukhtar, E.M.; et al. Ultrasound Imaging in subjects with sickle cell disease: The Saudi Arabia experiences. *Int. J. Gen. Med.* **2023**, *16*, 4931–4942.
26. Bureau, N.J.; Chhem, R.K.; Cardinal, É. Musculoskeletal infections: US manifestations. *Radiographics* **1999**, *19*, 1585–1592.

27. Pineda, C.; Vargas, A.; Rodríguez, A.V. Imaging of osteomyelitis: Current concepts. *Infect. Dis. Clin.* **2006**, *20*, 789–825.
28. Averill, L.W.; Hernandez, A.; Gonzalez, L.; Peña, A.H.; Jaramillo, D. Diagnosis of osteomyelitis in children: Utility of fat-suppressed contrast-enhanced MRI. *Am. J. Roentgenol.* **2009**, *192*, 1232–1238.
29. Dobaria, D.G.; Cohen, H.L. Osteomyelitis imaging. In *StatPearls [Internet]*; StatPearls Publishing: Treasure Island, FL, USA, 2023.
30. Miller, T.T.; Randolph, D.A., Jr.; Staron, R.B.; Feldman, F.; Cushin, S. Fat-suppressed MRI of musculoskeletal infection: Fast T2-weighted techniques versus gadolinium-enhanced T1-weighted images. *Skelet. Radiol.* **1997**, *26*, 654–658.
31. Kruk, K.A.; Dietrich, T.J.; Wildermuth, S.; Leschka, S.; Toepfer, A.; Waelti, S.; Waelti, S.; Kim, C.-H.O.; Güsewell, S.; Fischer, T. Diffusion-weighted imaging distinguishes between osteomyelitis, bone marrow edema, and healthy bone on forefoot magnetic resonance imaging. *J. Magn. Reson. Imaging* **2022**, *56*, 1571–1579.
32. Gilbert, B.R.; Cerqueira, M.D.; Eary, J.F.; Simmons, M.C.; Nabi, H.A.; Nelp, W.B. Indium-111 white blood cell scan for infectious complications of polycystic renal disease. *J. Nucl. Med.* **1985**, *26*, 1283–1286.
33. Foula, M.S.; Hassan, A.; AlQurashi, A.; Alsaihati, A.; Sharroufna, M. Spontaneous subgaleal hematoma in a patient with sickle cell disease: A case report and literature review. *Clin. Case Rep.* **2019**, *7*, 2220–2224.
34. Hanna, N.G.; Musleh, A.; Khan, H.; Chaudry, E.; Lahoud, C. Subperiosteal Orbital Hematoma: A Rare Clinical Manifestation of Sickle Cell Disease-A Case Report. *Case Rep. Ophthalmol.* **2023**, *14*, 388–393.
35. Saha, B.; Saha, A. Spontaneous epidural hemorrhage in sickle cell disease, are they all the same? A case report and comprehensive review of the literature. *Case Rep. Hematol.* **2019**, *2019*, 8974580.
36. Shah, D.; Reddy, H.; Kumar, S.; Acharya, S.; Reddy, H. Sickle cell disease presenting as extradural hematoma: An extremely rare fatal crisis. *Cureus* **2022**, *14*, e27004.
37. Guillin, R.; Moser, T.; Koob, M.; Khoury, V.; Chapuis, M.; Ropars, M.; Cardinal, E. Subperiosteal hematoma of the iliac bone: Imaging features of acute and chronic stages with emphasis on pathophysiology. *Skelet. Radiol.* **2012**, *41*, 667–675.
38. Kidwell, C.S.; Wintermark, M. Imaging of intracranial haemorrhage. *Lancet Neurol.* **2008**, *7*, 256–267.

Disclaimer/Publisher's Note: The statements, opinions and data contained in all publications are solely those of the individual author(s) and contributor(s) and not of MDPI and/or the editor(s). MDPI and/or the editor(s) disclaim responsibility for any injury to people or property resulting from any ideas, methods, instructions or products referred to in the content.